

## Random anisotropy models in the Ising limit

C. Jayaprakash

*Baker Laboratory, Cornell University, Ithaca, New York 14853  
and IBM Thomas J. Watson Research Center,\* Yorktown Heights, New York 10598*

S. Kirkpatrick

*IBM Thomas J. Watson Research Center, Yorktown Heights, New York 10598  
(Received 31 December 1979)*

We have performed Monte Carlo simulations on the random anisotropy axis model of Harris, Plischke, and Zuckermann (introduced to describe amorphous magnetic films such as Dy-Cu or Dy-Al) in the Ising-like limit of infinite anisotropy energy. The ground state of this model (studied in samples of up to  $20 \times 20 \times 20$  spins) exhibits significant short-range ferromagnetic order but no long-range magnetic order in three dimensions, supporting arguments of Pelcovits, Pytte, and Rudnick. The specific heat shows a narrow maximum but no obvious critical behavior. Relaxation studies provide evidence for a distinct stable low-temperature phase, but cannot determine whether a sharp phase transition occurs. The spin susceptibility at higher temperatures and magnetization as a function of field at low temperatures have been calculated. Although the absence of critical behavior in the specific heat of this model in zero field is reminiscent of some Ising spin-glasses, the magnetic behavior is indistinguishable from that of a ferromagnet with moderate coercivity.

### INTRODUCTION

To describe the unusual magnetic properties of amorphous intermetallic compounds containing non-S-state rare-earth ions, Harris, Plischke, and Zuckermann<sup>1-3</sup> have introduced a random anisotropy axis model or RAM. In these materials, magnetic ions with asymmetric charge distributions interact with their surroundings, giving rise to an anisotropy energy which in the low-symmetry amorphous environment will be of the easy-axis form. In amorphous substances, one expects that the preferred axis orientation will vary randomly from site to site with little correlation, a hypothesis which is supported by direct examination of computer models of amorphous metallic structures.<sup>3</sup> Finally, since the magnetic species are present in high concentration in these systems, the exchange interactions seen are predominantly ferromagnetic.

Harris *et al.* incorporated these ideas in the following model Hamiltonian:

$$\mathcal{H} = -J \sum_{\langle ij \rangle} \vec{S}_i \cdot \vec{S}_j - D \sum_i (\hat{n}_i \cdot \vec{S}_i)^2, \quad (1)$$

where  $\vec{S}_i$  is an  $n$ -component spin at site  $i$ ,  $J$  is the nearest-neighbor exchange-coupling constant, and the unit vector  $\hat{n}_i$  is the random easy-axis direction at site  $i$ . The  $\hat{n}_i$ 's are distributed independently and isotropically. Although Harris *et al.* intended to model the properties of amorphous TbFe<sub>2</sub>, the presence of two types of magnetic ions make that system more com-

plicated than Eq. (1). However, intermetallic compounds of rare earths such as Dy and nonmagnetic metals such as Al, Cu, and Ag have since received careful experimental study,<sup>2</sup> and this model has been applied to them.

Several authors have developed mean-field treatments of Eq. (1), and predicted phase diagrams on this basis,<sup>4-6</sup> with differing results. Harris and Zolbin<sup>4</sup> predicted a low-temperature ferromagnetic state for small anisotropy, characterized by the ratio  $D/J$ , and a spin-glass state for large  $D/J$ . Callen *et al.*<sup>5</sup> considered the ground state only in a mean-field analysis, and concluded that for all values of the relative anisotropy, the ground state was ferromagnetic. Numerical study of random local mean-field equations by Patterson *et al.*<sup>6</sup> gave similar predictions of ferromagnetism.

Monte Carlo calculations of the properties of Eq. (1) with classical spins and various ratios of  $D/J$ , carried out by Chi and various associates,<sup>7</sup> have given qualitative agreement with the magnetic phenomena, such as coercivity and remanance, observed for the amorphous alloys, but the resulting predictions about the nature of the low-temperature phase or phases have been ambiguous. Chi and Alben found the lowest-lying states were magnetic even in the limit of large  $D/J$ , but Chi and Egami subsequently applied a more elaborate computer algorithm and concluded that the ground states were nonmagnetic. Harris and Sung<sup>8</sup> have also simulated ground states of this model, and report a significant energy difference

between the lowest-lying spin-glass states and the ferromagnetic ground state.

Our interest in this model was stimulated by theoretical predictions that it should not be magnetic at all, and that mean-field theory should not apply. Aharony<sup>9</sup> has performed a  $4 - \epsilon$  renormalization-group expansion in the disordered phase, and found a "runaway" to either a spin-glass state or to some type of smeared transition. A simple argument gives a physical interpretation to this runaway.<sup>10</sup> Construct a ground state for Eq. (1) by dividing the system up into cells of linear dimension  $L$ . Let the spins be ferromagnetically aligned in each cell and oriented in a direction which maximizes the energy gained from the anisotropy term. The energy per spin gained in this way will be  $\propto DL^{-d/2}$ , while the exchange energy cost of the resulting random orientations, allowing for relaxation of any mismatch over a distance  $L$ , is  $\propto JL^{-2}$ . Below four dimensions a breakup into clusters is favored, with a characteristic cluster size of  $L_0 \propto (J/D)^{2/(4-d)}$ .

Thus the runaway is a crossover to Ising-like behavior in each cell, introducing on that scale some sort of two-level systems, or "instantons." The runaway depends only on the dimensionality of the system. Other factors, such as  $z$ , the coordination number of a spin, will influence only the coefficients in  $L_0$ . This argument leaves open the question of whether the cells have any preferred relative ordering. However, Chen, and Lubensky,<sup>11</sup> using the replica technique of taking averages, have derived an effective Hamiltonian for the large anisotropy limit of Eq. (1). It is identical to the effective Hamiltonian of an Ising spin-glass with random exchange interactions.<sup>12</sup>

Pelcovits, Pytte, and Rudnick (PPR)<sup>13</sup> have presented a variety of independent arguments which show that the ferromagnetic state is unstable below four dimensions, when the number of spin components is  $\geq 2$ . Using expansions in powers of  $D/J$  about the ferromagnetic state and the fact that  $\chi_1(q)$  remains gapless (i.e.,  $\propto q^{-2}$ ) to all order in  $D/J$ , they show that 4 is the lower critical dimensionality for model (1). Thus mean-field arguments cannot be relied upon to give the phase diagram in two or three dimensions.

A second reason for our interest in this model is that quite analogous technical problems and experimental uncertainties occur in spin-glasses. Massless "replicon"<sup>14</sup> modes cause instabilities in the spin-glass mean-field theory. The physical nature of these modes is a mystery, but they are a consequence of isotropy in the large scale, just as is the result,  $\chi_1(q) \propto q^{-2}$ , used by PPR. Similarly, some theoretical arguments suggest that  $d_c = 4$  for spin-glasses,<sup>14,15</sup> yet a rich variety of phenomena are observed in experiments on real materials as well as in computer experiments in 2D and 3D. Even if the spin-glass transition proves not to be sharp, but to be more like

the conventional glass transition, the profound differences between the low-temperature phase and a paramagnetic system need to be understood. We hope that close study of the borderline ferromagnetism which occurs in the RAM may provide some guidance for dealing with spin-glasses.

In this paper we concentrate on the Ising-like  $D \rightarrow \infty$  limit of model (1), since the experimental systems of interest are known from high-field magnetization studies<sup>16</sup> to have  $D/J \gg 1$ . It is not clear that the prediction by PPR of no ferromagnetism below four dimensions can be reconciled with the observed properties of, e.g., Dy-Cu films.<sup>17</sup> Finally, the  $D \rightarrow \infty$  limit permits different methods of calculation. To make the two-level systems explicit, we write

$$\vec{S}_i = \hat{n}_i \sigma_i \quad , \quad (2)$$

where  $\sigma_i = \pm 1$  and  $|\hat{S}|$  is set = 1 for convenience, and obtain

$$\mathcal{H} = \sum_{\langle ij \rangle} -J(\hat{n}_i \cdot \hat{n}_j) \sigma_i \sigma_j \quad . \quad (3)$$

This is a random-bond Ising model.

It has two soluble limiting cases. The infinite-ranged version, in which the sum in Eq. (3) extends over all pairs of spins, should give behavior appropriate to Eq. (3) in sufficiently high spatial dimensionality. This limit proves to be a ferromagnet. One-dimensional chains with the Hamiltonian (3) are easily solved, and have a nonmagnetic ground state, with only short-range magnetic order at  $T = 0$ . We describe these limits in Sec. II, and then present position-space renormalization-group arguments which suggest that the transition to ferromagnetic low-temperature behavior occurs at a finite critical dimensionality. Computer simulations are then used to study model (3) in two and three dimensions. In Sec. III, we consider ground-state properties of Eq. (3) in three spatial dimensions. Finite-temperature properties of the model in zero magnetic field are discussed in Sec. IV. In that section we make a qualitative comparison of certain time-dependent phenomena in the RAM with the same properties in systems known to have a phase transition. Section V reports magnetic properties of the system in an applied field. Our conclusions are collected and summarized in Sec. VI.

## II. LIMITING CASES

The infinite-ranged limiting case of Eq. (3), in which all pairs of spins are coupled,

$$\mathcal{H}_\infty = \sum_{i > j} -J(\hat{n}_i \cdot \hat{n}_j) \sigma_i \sigma_j \quad , \quad (4)$$

for  $1 \leq j \leq i \leq N$ , is an interesting case to study. This construction suppresses spatial variations in ordering by making all sites adjacent, and usually

results in a model for which the exact solution is identical to the mean-field-theory description of a finite-dimensional system with the same type of interactions. Thus it should describe the high dimensionality limit of Eq. (3). We shall now show that in this limit a ferromagnet is obtained.

Two cases will be of interest. If the original Hamiltonian (1) described Heisenberg spins ( $n=3$ ), it is most natural to assume that the  $\hat{n}_i$  are distributed over the unit sphere with uniform probability. If the spins in Eq. (1) are planar, or  $xy$  spins ( $n=2$ ), we shall assume the  $\hat{n}_i$  to be uniformly distributed over the unit circle. For convenience, we shall usually describe only the Heisenberg case. Since Eq. (4) can be rewritten

$$\mathcal{H}_\infty = \frac{1}{2} JN - \left(\frac{1}{2} J\right) \left| \sum_i \hat{n}_i \sigma_i \right|^2, \quad (5)$$

the energy depends only upon the magnitude of the magnetization. The lowest-energy states are those which maximize the total magnetic moment of the system.

A configuration which maximizes the magnetization along some chosen direction  $\hat{n}_0$  has all spins pointing in the same hemisphere or half-circle, with  $\hat{n}_0$  as the polar axis; i.e.,

$$\langle \hat{n}_0 \cdot \vec{S}_i \rangle > 0 \quad (6)$$

for all  $i$ . Different choices of  $\hat{n}_0$  give rise to at least  $N$  distinct configurations, one of which will be the ground state. The energies of the remaining states produced in this way deviate from the ground-state energy by relative amounts of order  $N^{-1/2}$ . Thus this set of low-lying states becomes, in the limit  $N \rightarrow \infty$ , an isotropic set of degenerate ground states. Thus, in contrast to classical vector spin models with no anisotropy, the entropy per spin vanishes at temperature  $T=0$  in the RAM as  $(\ln N)/N$ .

For each approximate ground state, defined by a choice of  $\hat{n}_0$  and the condition (6), an appropriate choice of the signs of the  $\{\hat{n}_i\}$  (which have no physical significance) makes all  $\sigma_i = +1$ . This is just a gauge transformation, in the sense Toulouse<sup>18</sup> has introduced, with each choice of  $\hat{n}_0$  corresponding to a natural global gauge for the description of the RAM. Mattis<sup>19</sup> has discussed random Ising models in which the ground state can be gauge transformed into a configuration with all  $\sigma_i$  equal. The model (4) shares that property, but it holds for each of its many ground states (in the limit  $N \rightarrow \infty$ ), which are not unique.

The spectrum of single spin-flip excitations from a ground state of Eq. (4) is given by the probability distribution of  $\cos(\theta_i) \equiv (\hat{n}_0 \cdot \vec{S}_i)$  over the hemisphere or half-circle. For the Heisenberg model, the distribution of  $\cos(\theta_i)$  is constant over the interval 0 to 1, while for planar spins the excitation density will be proportional to  $[1 - \cos(\theta_i)^2]^{-1/2}$ . In both cases, the density of zero-energy excitations is finite, so a specific-heat linear in  $T$  is expected. The ground-state energy per spin in Eq. (4) is given by  $\langle \hat{n}_i \cdot \hat{n}_j \rangle J$ . This is  $\frac{1}{4} J$  in the Heisenberg model, and  $4J/\pi^2 \approx 0.405J$  in the  $xy$  model. The ground-state moment  $\langle m \rangle$  is found by averaging  $(\hat{n}_0 \cdot \hat{n}_i)$  over a hemisphere or half-circle. The result is  $\langle m \rangle = \frac{1}{2} S$  for  $n=3$ , and  $(2/\pi)S \approx 0.637S$  for  $n=2$ .

Derrida and Vannimenus<sup>20</sup> have recently solved this model at nonzero temperatures, and for arbitrary values of  $D$ . Their results have a mean-field-like form, and exhibit a paramagnet-ferromagnet transition at  $T_c = J/n$ , where  $n$  is the number of spin components, for all values of  $D$ . They obtain a specific heat which is linear in  $T$  at low temperatures when  $D \rightarrow \infty$ .

In contrast to the isotropic, ferromagnetic, infinite-ranged RAM (4), the 1D version of this model is nonmagnetic, and has only twofold degeneracy in the ground state. The ground state can be constructed by aligning each spin with respect to its left-hand neighbor. If we choose a gauge in which all  $\hat{n}_i$  point in the same hemisphere, negative interactions will occur whenever two successive axes are more than  $90^\circ$  apart, as sketched in Fig. 1. For Heisenberg spins,  $1/\pi$  of the bonds are antiferromagnetic in this gauge, for  $xy$  spins,  $\frac{1}{4}$ . This causes the magnetization to tumble over as one moves along the chain in constructing the ground state, with the result that  $\langle m \rangle = 0$ .

Thomas<sup>21</sup> has recently published a solution for arbitrary temperatures of the 1D RAM in the limit  $D \rightarrow \infty$ . He finds that

$$\langle \langle \vec{S}_i \cdot \vec{S}_{i+n} \rangle \rangle = \langle \langle \vec{S}_i \cdot \vec{S}_{i+1} \rangle \rangle^n = \exp(-n/L_1) \quad (7)$$

where the double brackets denote averaging over the distribution of  $\{\vec{n}_i\}$  in addition to thermal averaging. In the ground state, for Heisenberg spins,  $L_1$  is found to be  $(\ln 2)^{-1} \approx 1.44$ , while for  $xy$  spins it is  $(\ln \frac{1}{2} \pi)^{-1} \approx 2.21$ . Since every bond is satisfied, the ground-state energy per bond is lower in 1D than in the infinite-range model (4). The resulting energy per bond is given by  $-\langle |\hat{n}_i \cdot \hat{n}_j| \rangle J$ , which is  $-\frac{1}{2} J$  for  $n=3$ , or  $-(2/\pi)J$  for  $n=2$ .



FIG. 1. Ground-state configuration of spins in a 1D RAM [see Eq. (4)]. Each spin is aligned with respect to its left-hand neighbor.

One dimension provides an extreme example of the destruction of ferromagnetic order through local fluctuations. Negative interactions between the  $\sigma_i$ 's defined in a particular gauge cause the average magnetization direction measured in the vicinity of a point far from the origin to execute a random walk over the surface of the sphere, soon leaving the vicinity of the direction,  $\hat{n}_0$ , chosen at the origin. A similar tendency is evident in 2D or 3D. If the  $\hat{n}_i$  are assigned to the sites of a lattice with all  $(\hat{n}_i \cdot \hat{n}_0) > 0$  for some choice of  $\hat{n}_0$ , the state with all  $\sigma_i = +1$  is certain to be unstable, since some of the spins will experience net negative exchange fields. The distribution of internal fields,  $h_i$ , where

$$h_i = \sum_j J(\hat{n}_i \cdot \hat{n}_j) \sigma_j \quad (8)$$

is half the excitation energy for a single spin flip, was found by sampling at sites of a 3D simple cubic lattice with Heisenberg spins and is shown in Fig. 2. Roughly one-fifth of the spins are initially unstable in this case, so the "asperomagnetic" picture<sup>22</sup> of a random ferromagnetic state with spin orientations confined to a hemisphere cannot hold in a finite-dimensional RAM. Further calculation is needed to determine whether this relaxation reduces  $\langle m \rangle$  to zero, or leaves it nonzero.

The position-space recursion relations introduced by Migdal<sup>23</sup> and generalized by Kadanoff<sup>24</sup> provide a way to estimate the effect of dimensionality in this model. The basic idea is that two spins  $b$  steps apart on a  $d$ -dimensional lattice will interact through of order  $b^{d-1}$  independent, or parallel,  $b$ -stepped paths. The prescription for a recursion relation in  $d$  dimen-

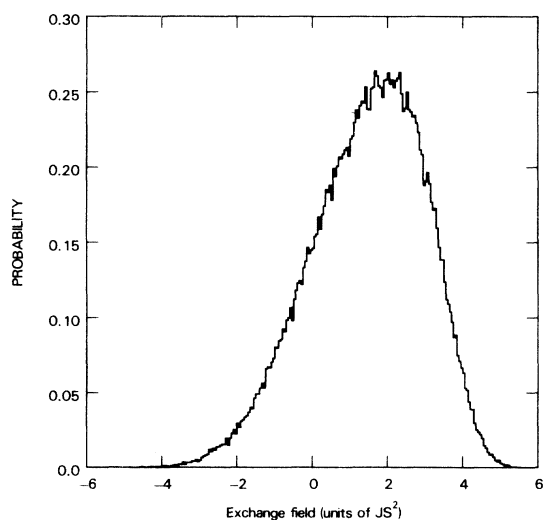


FIG. 2. Distribution of internal fields [see Eq. (7)] when all spins point in a given hemisphere. Data are averaged over 20 samples of  $20 \times 20 \times 20$  spins each. Note that a large fraction of spins experience destabilizing fields.

sions is, therefore, to take  $b$  bonds in series, couple groups of  $b^{d-1}$  of them in parallel, and use the resulting new interactions as input to the next stage. In the low-temperature limit, the strength of  $b$  exchange interactions in series is the magnitude of the weakest interaction in the chain. The sign of the combined interactions is the product of the signs of the constituents.<sup>25</sup> To combine several chains in parallel, one simply adds their interaction strengths.

Once a gauge,  $\hat{n}_0$ , has been fixed, the bonds  $J_{ij} \equiv J(\hat{n}_i \cdot \hat{n}_j)$  are distributed between  $-J$  and  $J$  with weight  $P(J_{ij}) = (2J)^{-1} + (\pi J)^{-1} \sin^{-1}(J_{ij})$  (for  $n=3$ ), and have average strength  $\frac{1}{4}J$ , ferromagnetic in sign. Taking two such bonds in series gives

$$J_{ik} = J \operatorname{sgn}[(\hat{n}_i \cdot \hat{n}_j)(\hat{n}_j \cdot \hat{n}_k)] \min[|\hat{n}_i \cdot \hat{n}_j|, |\hat{n}_j \cdot \hat{n}_k|] \quad (9)$$

decreasing the average bond strength to  $0.1J$ . Taking  $m$  chains in parallel increases the average interaction strength  $m$ -fold. For two two-stepped chains in parallel, as is appropriate to a two-dimensional lattice, the result is still less ferromagnetic than the original bonds. For 3D, four two-stepped chains in parallel have an average strength of  $0.4J$ , more ferromagnetic than a single bond. The distribution of bond strengths which results from summing Eq. (9) over four intermediate sites, holding the two end sites fixed, is compared in Fig. 3 with the original distribu-

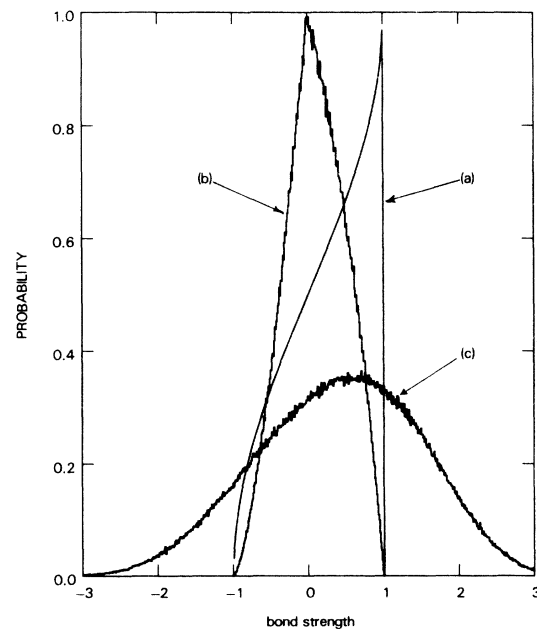


FIG. 3. Three distributions of low-temperature bond strengths for the random-axis model, each for a sample of 960 000 bonds. Plotted are (a) individual bonds, (b) chains of two bonds each [obtained from Eq. (8)], and (c) sets of four parallel two-bond chains.

tion of interactions for a single bond of the RAM. The Migdal procedure therefore suggests that there will be long-range ferromagnetic order in the 3D RAM, but only short-range correlations in 2D.

The prediction that the  $D \rightarrow \infty$  RAM (3) is ferromagnetic at low  $T$  above some critical dimensionality,  $d_c$ , is a plausible result, given the properties of the infinite-ranged limit (4). We are skeptical, however, of the conclusion that  $d_c$  lies between 2 and 3, since the Migdal-Kadanoff recursion in effect shifts bonds from their actual locations, and does not respect frustration.<sup>25</sup> We find that 0.40 of the elementary square plaquettes are frustrated in model (3) for Heisenberg spins, regardless of dimensionality. [If the same fraction ( $\frac{1}{4}$ ) of antiferromagnetic bonds were present but uncorrelated in their positions, 0.42 of the plaquettes would be frustrated. The fact that the random bonds are derived from the random angles defined at the sites distorts the frustration statistics only slightly.] In studies of 3D random-bond Ising models in which the sign of a fraction of the bonds was reversed without changing their strengths, ferromagnetic order was found to be destroyed when roughly 0.35 of the plaquettes were frustrated.<sup>26</sup> In the RAM, the negative bonds are, on the average, weaker than the ferromagnetic bonds, so the loss of ferromagnetic order should require a greater degree of frustration. In the light of the studies of spin-glasses, and the position-space renormalization-group arguments presented here, it is at least possible that the RAM is a ferromagnet in 3D, and quite likely that it is ferromagnetic for all  $d \geq 4$ .

### III. NUMERICAL STUDIES—GROUND STATE

The ground state of the RAM for Heisenberg spins on 3D simple-cubic lattices was studied by computer simulation. Samples were created by assigning values of the  $\hat{n}_i$  with a random number generator, allowing  $n_i^x$  to be uniformly distributed between 0 and 1, while the azimuthal angle varied uniformly between 0 and  $2\pi$ . Each sample was then cooled slowly, starting from a random configuration of  $\{\sigma_i\}$ , using standard Monte Carlo techniques.<sup>27</sup> Once cooled, samples were repeatedly warmed to moderate temperatures and cooled again, sometimes subjected to small external fields, while the lowest-energy states and the associated moments were monitored. We searched exhaustively for single- and two-spin flips which lowered the energy of the sample, and permitted flips of four spins at the corners of a plaquette. This gave no significant further energy lowering, nor did it modify any spin correlations significantly. Correlation functions  $\langle \vec{S}_i \cdot \vec{S}_{i+n} \rangle$  were obtained for each ground state, using the actual spins defined by Eq. (2). One sample of  $20 \times 20 \times 20$  sites was studied extensively at higher temperatures as well as near its

ground state, accounting for more than 20 hours of computing on an IBM 370/168, or about  $4 \times 10^5$  Monte Carlo time steps per spin (since each attempted spin flip requires about  $25 \mu\text{sec}$ ). Results for this sample are reported in this and Secs. IV and V. Smaller samples, several each with  $16^3$ ,  $12^3$ ,  $10^3$ , and  $8^3$  sites, were also considered, since significant size dependences were found in the low-temperature properties.

The ground-state energy of the RAM with Heisenberg spins on the 3D simple cubic lattice was found to be  $-1.11 \pm 0.02J$  per spin. This translates into  $-0.37J$  per bond, almost exactly halfway between the results,  $-\frac{1}{4}J$  and  $-\frac{1}{2}J$ , found in the infinite-range limit and the 1D case, respectively. It indicates that a significant amount of local relaxation away from the ferromagnetic state has taken place.

A second measure of the extent of relaxation away from the ferromagnetic state is the internal field distribution. Figure 4 contrasts the distribution of  $h_i$  found in the ground state of our  $20 \times 20 \times 20$  site sample with the unrelaxed distribution from Fig. 2. The density of single spin-flip excitations,  $P(h)$ , is maximum at  $h = 2J$ , and decreases to one fourth its maximum value as  $h \rightarrow 0$ . The nonvanishing density of excitations at zero energy implies that the specific heat of this model will have a contribution linear in  $T$ , although the Schottky anomaly associated with the larger density of excitations around  $h = 2J$  may disguise the linear term at most accessible temperatures. Using the data in Fig. 4, we estimate that the contribution to the specific heat from single spin-flip exci-

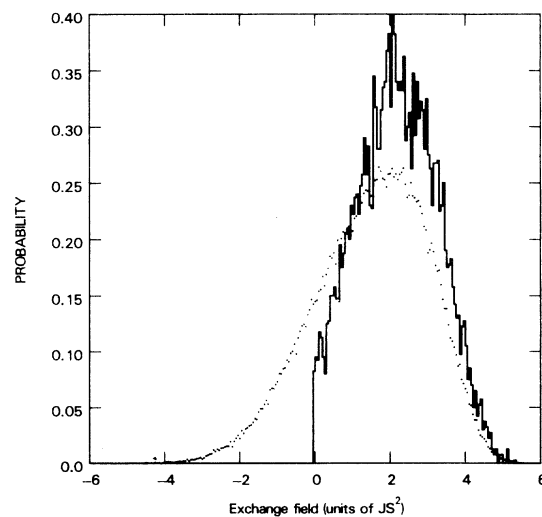


FIG. 4. Distribution of internal fields in the ground state of a  $20 \times 20 \times 20$  sample. For comparison the ferromagnetically aligned case shown in Fig. 2 is dotted in.  $P(h)$  is finite at  $h = 0$ .

tations in this model is roughly

$$C(T) \approx 0.1(T/J) + 0.225(T/J)^2. \quad (10)$$

The relaxed internal field distribution shown in Fig. 4 is not a sensitive function of sample size. Rather similar distributions were obtained in samples of the RAM with  $16^3$ ,  $12^3$ , and  $8^3$  sites. In particular, the characteristic feature that  $P(h=0) \approx 0.25P_{\max}$  is obtained in all four sample sizes. In contrast to the situation in systems with longer-ranged interactions,<sup>28,29</sup> which act to reduce  $P(h=0)$  to zero,  $P(h)$  for the RAM appears not to depend upon any cooperative effects. It is therefore likely that an appropriately constructed cluster model can give a good account of the low-temperature thermal properties of the RAM.

To determine whether the model is ferromagnetic or not we have calculated spin-correlation functions  $G(R) \equiv \langle \vec{S}_i \cdot \vec{S}_{i+R} \rangle$  for the  $20 \times 20 \times 20$  site sample as well as for several smaller samples in their ground states. These results, averaged over all pairs of spins displaced by a given number of steps along a cube axis, are plotted in Fig. 5. The nearest-neighbor correlation function, like the ground-state energy, is insensitive to sample size, but the decay of correlations at greater distances proves extremely sensitive. In a sample of  $8^3$  sites,  $G(R)$  decreases only to  $\approx 0.08$  at a separation of 4 sites before the periodic boundary conditions cause it to increase again.  $G(R)$  decreased only slightly further in a  $12^3$  site sample. Samples with  $16^3$  and  $20^3$  sites were large enough, however, that  $G(R)$  decreased to zero

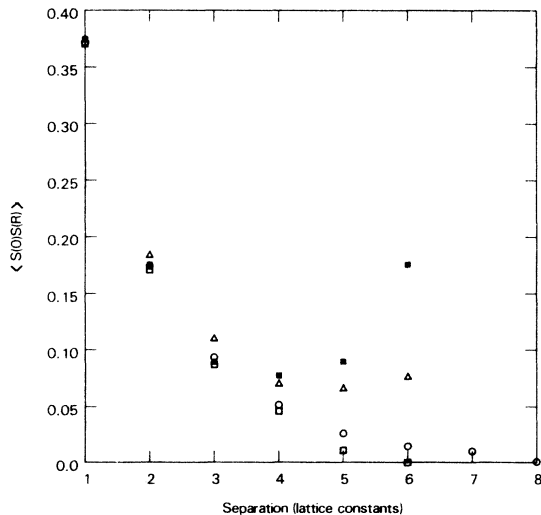


FIG. 5. Spin-spin correlations in the ground state of the RAM, averaged over pairs of spins along a cube axis, for samples of various sizes: circles correspond to  $20 \times 20 \times 20$ , open squares to  $16 \times 16 \times 16$ , open triangles to  $12 \times 12 \times 12$  and squares to  $8 \times 8 \times 8$ . Note the evidence for short-range ferromagnetic order.

within numerical uncertainty. Repeating the calculations of  $G(R)$  on a different sample with  $20^3$  spins, we reproduced the results in Fig. 5 to within  $\pm 0.02$ . The decay length analogous to  $L_1$  which one infers from Fig. 5 is approximately 1.5, not significantly greater than its value for the 1D case.

We conclude, therefore, that there is a threshold sample size necessary for accurate numerical investigation of the RAM. Samples of linear dimension 10 or 12 may well appear ferromagnetic, especially if the anisotropy coefficient,  $D$ , is not taken to be infinite, but larger samples will have more of the characteristics of a spin-glass. The samples studied by Chi *et al.*<sup>7</sup> and by Harris and Sung<sup>8</sup> had only of order 1000 sites each. We suspect that the difficulty these authors encountered in determining the nature of the true ground state was a consequence of the small sample sizes employed.

In studying the low-lying states of RAM's of various sizes we observed this sort of threshold size effect. The lowest-energy states of samples with linear dimensions 8–12 sites tended to be weakly magnetic, with magnetizations some 20% of the maximum possible. Larger samples, 16 or 20 sites on a side, had moments of only 1 to 3% of the maximum in their ground states. In all cases, however, states with greater magnetization could be obtained with very little cost in exchange energy, typically  $< 0.1J$  per spin above the ground state. We discuss these easily magnetized states further in Sec. V.

#### IV. FINITE-TEMPERATURE PROPERTIES IN ZERO FIELD

The thermodynamic properties of our  $20^3$  sample were determined by Monte Carlo runs at finite temperature, with and without an external field term coupling to the  $\vec{S}_i$ . The results for the zero-field case are reported in this section. Care was taken to average the data over very long times to ensure precision. Typically, 10 000 Monte Carlo time steps per spin (MCS) were used for each temperature low enough ( $kT \leq 1.5J$ ) that there was evidence for magnetic order beyond immediate neighbors.

The internal energy of the  $20^3$  spin Heisenberg model is plotted in Fig. 6. In the infinite-ranged RAM with  $D \gg J$  and Heisenberg spins, the internal energy is zero<sup>20</sup> above the transition temperature. (The analogous mean-field ferromagnetic transition temperature for the 3D RAM would be  $kT/J = \frac{1}{3}z = 2$ .) Below this critical temperature,  $U(T)$ , in units appropriate for comparison with our 3D results, decreases to  $-0.75J$ . The observed  $U(T)$  in 3D is lower at all temperatures, as a consequence of local relaxation away from the ferromagnetic state. A more interesting comparison can be made with the

internal energy in the 1D RAM,

$$U_{1D}(T)/J = -\left(\frac{1}{2}z\right) \langle \tanh(\hat{n}_i \cdot \hat{n}_j/kT) \rangle . \quad (11)$$

This is also the one-bond, or lowest order contribution to the internal energy in the usual high-temperature expansion of the free energy for model (3). It is indicated by the solid line in Fig. 6. In 3D, ferromagnetic short-range order, which suppresses thermal fluctuations, causes  $U(T)$  to decrease more rapidly than the 1D curve. Since at the lowest temperatures, not all bonds are satisfied, frustration (which is absent in the 1D case) increases the ground-state energy to  $-1.11J$  instead of  $-1.5J$ . This effect is first seen near  $T = 1.25$ , where  $U(T)$  begins to saturate in the 3D model.

Direct examination of  $G(R, T)$  supports this interpretation of Fig. 6. In Fig. 7 we show  $G(R, T)$  for spins separated along the  $(0,0,n)$  axis, at temperatures of 0.05, 1.0, 1.2, and 2.0 $J$ . At  $kT = 1.2J$ , magnetic nearest-neighbor correlations are decreased by only 25% or so from their zero-temperature values. However,  $G(R)$  is changing rapidly with temperature, for roughly half of the decrease in each correlation occurs in the temperature range from  $T = 1.0J$  to 1.2 $J$ . By  $T = 2.0$ ,  $G(R)$  has become much shorter ranged. The correlations prove to be reasonably isotropic. Data from different symmetry axes, when

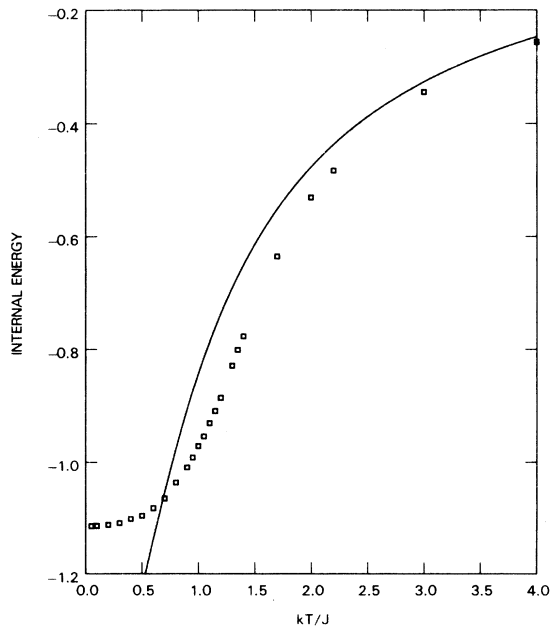


FIG. 6. Internal energy of a  $20 \times 20 \times 20$  sample of the RAM in the Ising limit as a function of the temperature  $T$ . Data are averaged over 7500 MCS or more. The solid line indicates three times the internal energy of a 1D RAM. Frustration accounts for the increase in the internal energy at  $T = 0$ .

plotted against separation distance, fall on the same curves as the data in Fig. 7.

The specific heat obtained for our largest sample, and as averaged over several smaller samples, is shown in Fig. 8. At the lowest temperatures, the data increase linearly or slightly faster with temperature. Using the excitation spectrum  $P(h)$  plotted in Fig. 4, we can estimate the contribution of single spin-flip excitations to  $C(T)$ .  $P(h)$  was approximated as a constant contribution extending from  $h = 0$  to  $4J$ , plus an isosceles triangle, with the same width and three times the height of the constant background. The contribution to  $C(T)$  from these processes, given by (10), is indicated in Fig. 8 by a dashed line. Almost all of  $C(T)$  is accounted for in this way at temperatures  $\leq J$ .

We can also use this formula to make contact with experiments on Dy-Cu films. Data on Coey *et al.*<sup>7</sup> are compared with this low-temperature prediction in Fig. 9, and fairly good agreement is obtained. To fix the temperature scale ( $T/J$ ) in Fig. 9,  $JS^2$  for the Dy-Cu film was extracted from the high-temperature susceptibility ( $\theta = 19.7$  K). The film for which the data in Fig. 9 is plotted had a concentration of about 48 at. % Dy, which implies an average coordination number of about 6, so our 3D sc lattice data should be applicable without further adjustment. The good agreement obtained shows that the Ising-like degrees

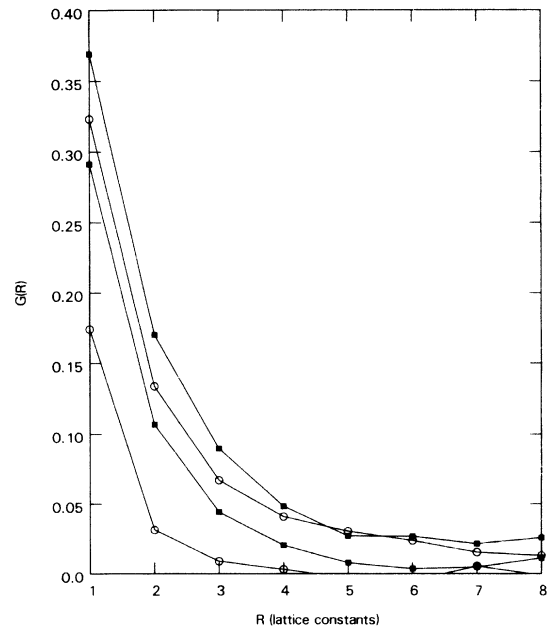


FIG. 7. Spin-spin correlations in a  $20 \times 20 \times 20$  RAM at temperatures of 2.0, 1.2, 1.0, and 0.05 $J$ . The spatial separation  $R$  is  $n$  steps along the  $[001]$  direction. Observe the marked decrease in the extent of correlation at  $T = 2.0J$ , in contrast to the behavior up to  $T = 1.2J$ .

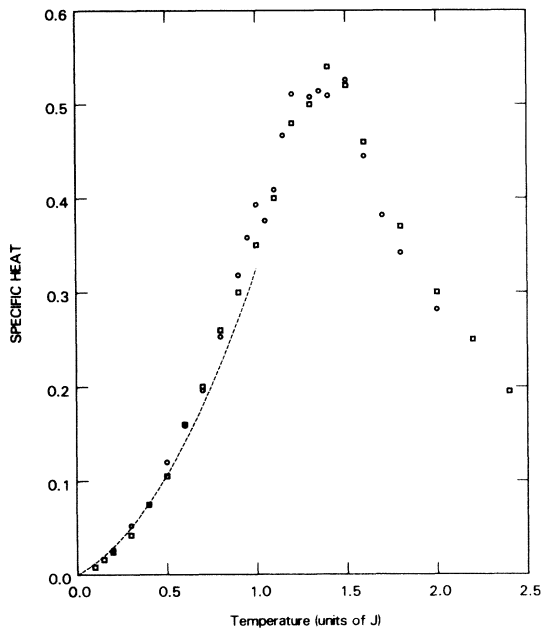


FIG. 8. Specific-heat data for a  $20 \times 20 \times 20$  sample of the infinite random anisotropy model (circles), and for  $12 \times 12 \times 12$  samples (squares). Dashed line indicates contribution of single spin reversals, calculated using  $P(h)$ . The maximum value of the specific heat shows no size dependence.

of freedom do in fact dominate the thermodynamics of this system at low temperatures. However, the  $P(h)$  curves which explain the low-temperature specific heat were not sensitive to sample size. Thus the low-temperature excitations observed through the specific-heat measurement are relatively local. They give no direct information about the nature of

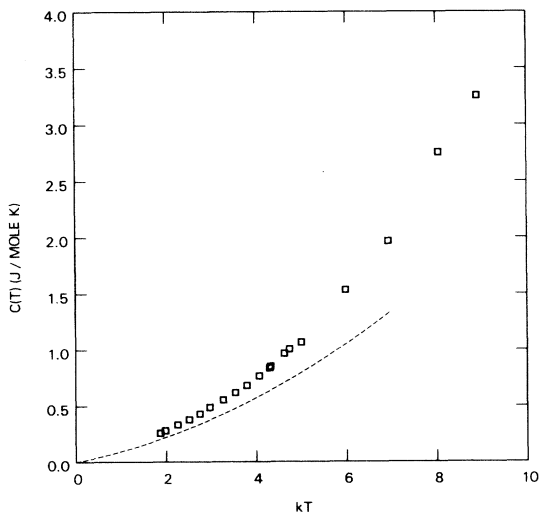


FIG. 9. Data from Ref. 9 for  $\text{Dy}_{0.48}\text{Cu}_{0.52}$ . The dashed line represents our results for the Ising limit of the random-axis model, with the temperature scaled appropriately.

cooperative effects over large scales which might occur close to the freezing temperature.

There is a rather narrow rounded maximum in  $C(T)$  at  $T=1.3J$ . Such a maximum, seen at the ordering temperature of a more conventional system, might be rounded due to finite size effects. As a test for critical behavior, we compared curves for  $C(T)$  obtained on several sizes of samples.  $C(T)$  in a conventional ferromagnet sharpens up perceptibly as the sample size is increased. This does not occur in Fig. 8. The same temperature appears to be the freezing temperature by more intuitive criteria. [ $U(T)$  begins to saturate, as discussed above, and some slowing of equilibration times occurs, as discussed below.] But there is no evidence for any critical singularity in the specific heat near  $T=1.3J$ , just as is the case in spin-glasses.<sup>30</sup> There is a faint possibility that a weak upwards cusp occurs in  $C(T)$  at  $T \approx 0.7J$ , and sharpens slightly with increasing sample size. This might result if the specific-heat exponent  $\alpha = -1$ . But there appear to be no associated freezing effects unique to that range of temperatures.

We have also studied the 2D square lattice, with planar spins, and anisotropy axes which are uniformly distributed in angle in the plane of the spins, again taking the Ising-like limit. Our observations for  $C(T)$  are shown in Fig. 10. The curve is quite similar in form to the 3D results. The maximum is rounded (and insensitive to sample size), and the

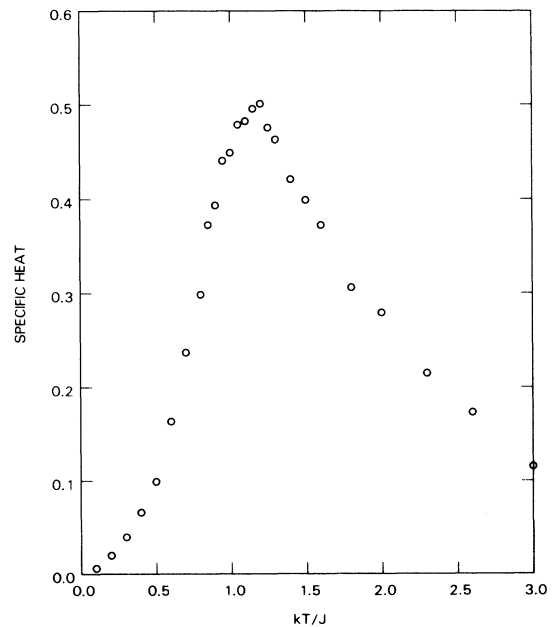


FIG. 10. Specific-heat data for a 2D RAM ( $64 \times 64$  sample), with  $xy$  spins and random circular anisotropy. Up to 15000 MCS were taken in the vicinity of the peak. Qualitative features resemble those for the 3D RAM with  $n=3$  spins shown in Fig. 8.

low-temperature region appears to contain both  $T$  and  $T^2$  contributions.

We have examined the time dependence of the energy density in our Monte Carlo calculations to distinguish between low- and high-temperature behavior. For each measurement the system was first equilibrated at some temperature  $T_1$ , say  $1.7J$ , for up to 1000 MCS, using samples of up to  $30 \times 30 \times 30$  sites.  $T$  was then changed to a nearby value,  $T_2$ , say  $1.4J$ , and the energy monitored as a function of time as the new equilibrium was approached. This was done for both  $T_1 > T_2$  and  $T_1 < T_2$ , for pairs of temperatures above the apparent freezing temperature, near it, and below it. The resulting energy relaxation curves are displayed in Fig. 11(a). The temperature differences  $|T_1 - T_2|$  were chosen to make the resulting change in internal energy of order  $0.1J$ . The short-time behavior is perceptibly temperature dependent. The time for the energy to reach a steady state value is short at high temperatures, longer in the vicinity of  $T \approx 1.3J$ , and short again at low temperatures ( $T < J$ ). The relaxation time obtained in this way increases slightly with increasing sample size near  $T \approx 1.3J$ , but is insensitive to sample size at higher or lower temperatures.

For comparison, we have performed similar observations on two systems known to have conventional phase transitions, with divergent correlation lengths. Curves for the 2D Ising ferromagnet, which has a transition at  $T = 2.3J$ , are shown in Fig. 11(b). Critical slowing down causes the lengthening of the equilibration time at  $T \approx 2.2J$  in the 2D magnet. At lower temperatures, in the ordered phase, equilibration again occurs rapidly. The equilibration of the 1D Is-

ing ferromagnet, which has a transition at  $T = 0$ , is studied in Fig. 11(c). In this case, the equilibration time increases monotonically with decreasing temperature.

The increasingly rapid equilibration seen in the RAM below  $T \approx 1.3J$  suggests that there is a distinct stable phase at low temperatures, in contrast with the 1D system, which orders only at  $T = 0$ . We have seen similar behavior in spin-glasses with bonds of random sign but constant strength (unpublished). This evidence conflicts with the recent proposal of Moore and co-workers<sup>14</sup> that spin-glass ordering (and by extension the nonmagnetic low-temperature phase of the RAM) is a kinetic effect due to long equilibration times. Although they suggested that the 1D Ising ferromagnet would provide a good analogue to the behavior of a spin-glass at low temperatures, Figs. 11 show that the approach to equilibrium is much more rapid in the RAM, at least over short and moderate time scales.

Dynamical observations like those in Fig. 11 probe only short time scales (of order  $10^{-6}$  to  $10^{-9}$  sec in the physical system being simulated), and cannot distinguish long-lived metastable states from equilibrium. Figure 11(a) suggests a transition like a glass transition, but does not rule out a sharp phase transition which exhibits no critical slowing down in the nonequilibrium energy relaxation time. Calculations by one of us<sup>31</sup> on spin-glasses with interactions of random sign have found weak slowing down of the energy relaxation times close to the freezing temperature, although the relaxation time determined from the decay of magnetization fluctuations in equilibrium does exhibit marked critical slowing down.<sup>32</sup>

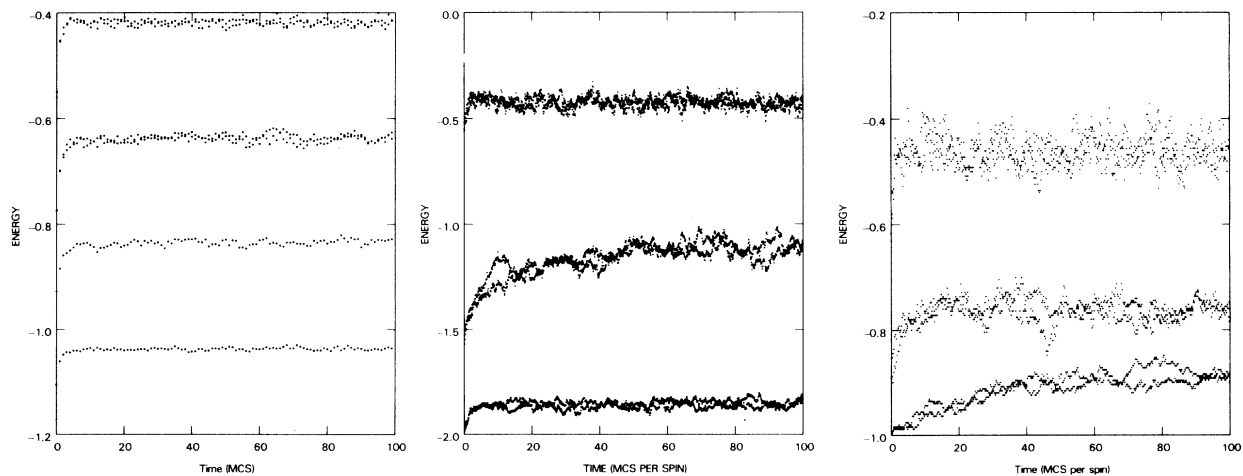


FIG. 11. (a) Equilibration of the internal energy in a  $30 \times 30 \times 30$  spin RAM after a sudden increase in temperature. The temperature changes studied were  $0.3-0.8$ ,  $1.1-1.3$ ,  $1.4-1.7$ , and  $1.9-2.5J$ . The system was allowed to equilibrate at the first temperature for 400 MCS before each curve was taken. (b) Equilibration curves, analogous to (a), for a  $60 \times 60$  spin Ising ferromagnet at temperatures  $1.3-1.8$ ,  $2.2-2.5$ , and  $4.0-5.0J$ . (c) Equilibration curves, analogous to (a), for a 1D Ising ferromagnet with 1000 spins. The temperature pairs studied in (c) are  $0.4-0.7$ ,  $0.7-1.0$ , and  $1.4-2.0J$ .

### V. MAGNETIC PROPERTIES

Model (1) was originally proposed to account for anomalous magnetic properties, in particular the temperature dependence of the coercive field, in amorphous rare-earth-iron alloys. In this section, we report results of our calculations of the magnetic-field-dependent properties of the random axis model with Heisenberg spins and anisotropy axes uniformly distributed over the surface of the sphere. Chi and Alben<sup>7</sup> have obtained hysteresis loops from computer simulations at zero temperature for various values of  $D$ , the anisotropy constant. Our calculations for this model complement theirs by providing information at finite temperatures, in the limit of  $D \gg J$ . The results of this section should be comparable with experiment, if the RAM is in fact an appropriate model for the rare-earth alloys.

Hysteresis loops, remanent magnetizations, and coercive fields were obtained on  $16 \times 16 \times 16$  spin samples, large enough to have nonmagnetic ground states. In Fig. 12 we show results obtained at  $T = 0.3J$  and  $0.8J$  (magnetization and demagnetization curves only). The data were obtained by cooling the sample in the absence of a field, then changing the field in steps of  $0.1J$  while allowing 1000 MCS for equilibration at each value of field. At temperatures above roughly  $1.2J$ , the magnetization is reversible on this time scale, and a longitudinal susceptibility

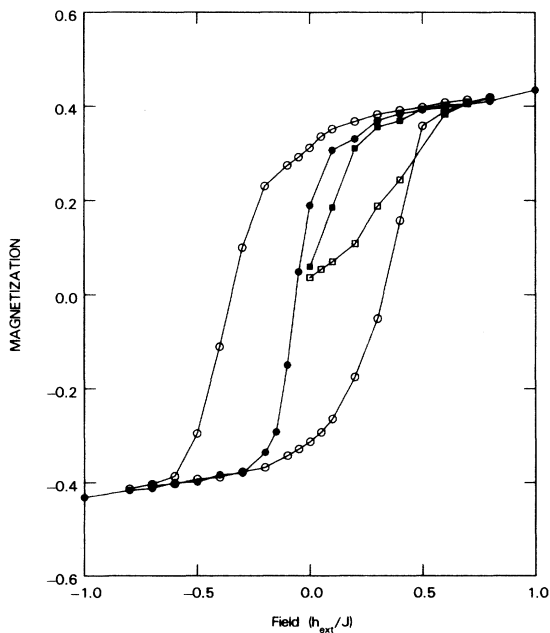


FIG. 12. Hysteresis loops for the RAM at temperatures of  $T = 0.3$  (open data points) and  $T = 0.8$  (solid points). The sample contained  $16 \times 16 \times 16$  spins, and was cooled in zero field for the start of each case. For each point, 1000 MCS were taken.

can be defined. Observation of hysteresis below  $1.2J$  is consistent with our identification of  $T \approx 1.3J$  as the freezing temperature  $T_f$ . By the usual experimental criteria, this model can be said to have a spontaneous moment below  $T_f$ , even though we find that the lowest energy states are nonmagnetic. The differential susceptibility in finite fields is nonlinear. Even at low temperatures, fields in excess of  $J$  are required for the magnetization to approach its saturation value,  $0.5S$  per spin.

This magnetic behavior contrasts with the  $M(h)$  characteristics one obtains for a uniform Ising ferromagnet on the same time scales. In the uniform system, the hysteresis loops are square, rather than rounded as in Fig. 12. The experimental literature on rare-earth intermetallic amorphous films reviewed in Ref. 2 contains many examples of hysteresis curves which are rounded like Fig. 12. The coercive fields of the amorphous films are relatively low at most temperatures. By contrast, even close to the ordering temperature in the uniform Ising system, fields comparable to  $J$  in strength must be applied to obtain reversal of the metastable magnetization in times less than 1000 MCS.

To show the evolution of the hysteretic behavior of the RAM with decreasing temperature we collect demagnetization curves for temperatures  $1.2, 0.8, 0.6, 0.4, 0.2$ , and  $0.05J$  in Fig. 13. In each case the sample was cooled to that temperature in a field of

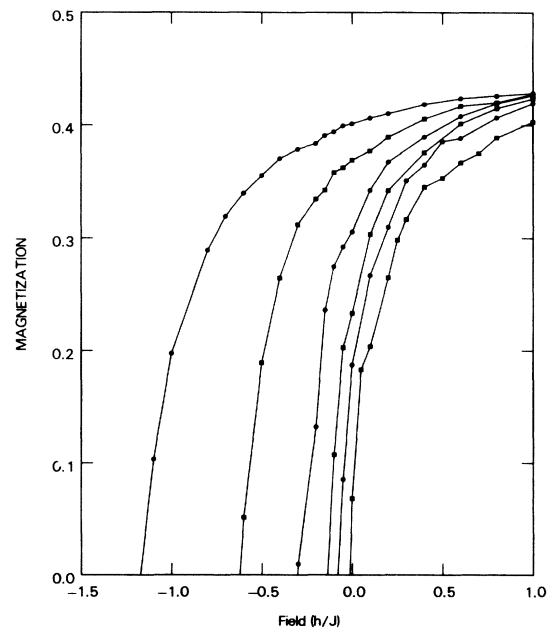


FIG. 13. Demagnetization curves for a  $16 \times 16 \times 16$  sample of the RAM. The sample was cooled in a field of  $1.0J$  to temperatures of (left to right)  $0.05, 0.2, 0.4, 0.6, 0.8$ , and  $1.2J$ , before decreasing the field. 800 MCS of equilibration were taken for each point plotted.

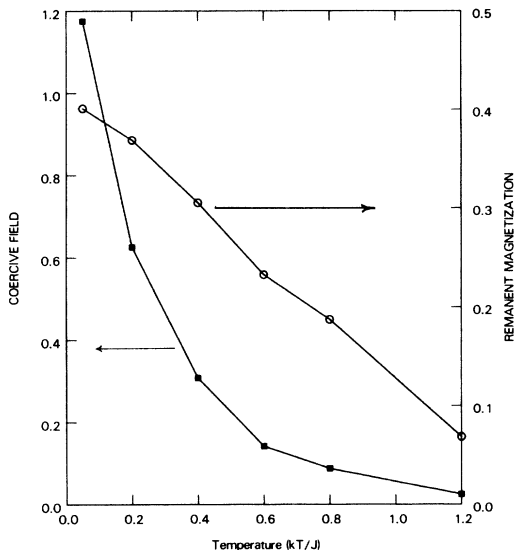


FIG. 14. Remanent magnetization (the zero-field intercept) and coercive field (zero-magnetization intercept) as a function of temperature, extracted from the data in Fig. 13 for the 3D random-axis model.

$1.0J$ . The field was then reduced in steps of  $0.1$  or  $0.05J$ , allowing 800 MCS for equilibration at each field value. The curves remain rounded to the lowest temperature studied.

The intercepts of the curves in Fig. 13 are plotted in Fig. 14. As is seen experimentally,<sup>2</sup> the magnetization increases smoothly to its limiting low-temperature value, while the coercive field remains small down to temperatures roughly one-third of  $T_f$  before increasing dramatically. For large  $D/J$ , Chi and Alben<sup>7</sup> observed a coercivity of roughly  $0.2zJ$  ( $z=6$  in our case) at  $T=0$ . This agrees with the largest coercive field plotted in Fig. 14.

## VI. CONCLUSIONS

In this investigation we have attempted to clarify the properties of the random axis model (1) by restricting attention to its extreme case,  $D \rightarrow \infty$ . Our results support the hypothesis that the limiting model (4) is a ferromagnet in sufficiently high spatial dimensionalities, but is a spin-glass with short-range ferromagnetic correlation in 3D. This confirms Pelcovits, Pytte, and Rudnick's prediction<sup>13</sup> that ferromagnetism is unstable in the 3D random axis model. Reference 13 leaves open the question of whether the RAM becomes ferromagnetic in sufficiently high dimensionality when  $D$  is large. The discussion of the infinite-range limit, which has a manifestly ferromagnetic ground state, suggests that it does. In addition we find, within the uncontrolled approximations of position-space rescaling, that the

model becomes ferromagnetic above some relatively low spatial dimensionality. A Migdal-Kadanoff recursion procedure gives a crossover between 2D and 3D. We speculate that in fact ferromagnetism is stable above 4D for any  $D$ .

Previous numerical studies<sup>7,8</sup> of the 3D RAM have come to varying conclusions, some arguing for a ferromagnetic, others for a spin-glass phase at low temperatures. We conclude that the observations of ferromagnetic behavior were an artifact of significant short-range ferromagnetic correlations in small samples. For many purposes, simulations in samples of 20 sites on a side appear to be adequate. Naive domain formation arguments suggest that the characteristic length for ferromagnetic correlations goes to zero as  $D \rightarrow \infty$ . However, the exactly soluble 1D example shows that a characteristic length of 1–2 sites persists for values of  $D$  large enough to restrict the spins to have only Ising-like degrees of freedom. We find a comparable persistence of short-range order in 3D.

Several connections can be made between this work and recent studies of models of spin-glasses. Ising systems with bonds of randomly varying signs, a class of models including both the RAM and the most commonly studied spin-glasses, have nonmagnetic 1D ground states which can be constructed trivially. There are also similarities between the RAM and spin-glasses in the infinite-range limit, since both have the unusual feature (for Ising models) of having highly degenerate ground states. The ground states of the RAM in the infinite-ranged limit can conveniently be labeled by the direction of their magnetization. The spin-glass ground states have no analogous natural label. The magnetization in the RAM is useful in characterizing the instability of the ferromagnetic state below 4D. The instability occurs as a direct consequence of frustration, as different ground states are preferred in different spatial regions. It remains to be seen whether any similar local characterization of locally rigid regions, or clusters, can be constructed for spin-glasses. However, the spin-glass is a more difficult problem in another way. Mean-field theory breaks down for it in the infinite-range limit, while in the infinite-range RAM the frustration is irrelevant.

The RAM is quite successful in reproducing the magnetic properties of the class of amorphous ferromagnetic films it was intended to model. The magnetization increases slowly over a wide range of temperatures below  $T_f$ , rather than rapidly within a narrow critical region, as would be seen in a uniform ferromagnet. The coercive field increases even more slowly at first, but then becomes quite large at temperatures well below the freezing temperature. Hysteresis loops in the RAM are rounded at low temperatures.

Zero-field static properties are also in qualitative

agreement with experiment. The specific heat at low  $T$ , calculated by taking only single spin flips into account in the large  $D$  limit, agrees to within 20% with the low-temperature data of Coey *et al.*<sup>17</sup> for  $\text{Dy}_{0.48}\text{Cu}_{0.52}$ . The Dy-Cu films have such small volumes that the peak in the magnetic specific heat could not be resolved experimentally and compared with our theory. However, Wenger and Keesom<sup>30</sup> found that the specific-heat maximum in classical spin-glasses contains no sharp features, just as we observe for the RAM.

#### ACKNOWLEDGMENTS

We thank B. Derrida and J. Vannimenus for discussions and for communicating their work (Ref. 20) to us before publication. Detailed comments by Professor M. E. Fisher on a preliminary version of this manuscript and discussions with G. Grinstein and H. Thomas are also gratefully acknowledged. One of us (C.J.) has been supported in part by the National Science Foundation.

\*Portions of this work were carried out while a visitor at IBM.

- <sup>1</sup>R. Harris, M. Plischke, and M. J. Zuckermann, *Phys. Rev. Lett.* **31**, 160 (1973).
- <sup>2</sup>R. W. Cochrane, R. Harris, and M. J. Zuckermann, *Phys. Rep.* **48**, 1 (1978).
- <sup>3</sup>R. W. Cochrane, R. Harris, M. Plischke, D. Zobin, and M. J. Zuckermann, *J. Phys. F* **5**, 763 (1975).
- <sup>4</sup>R. Harris and D. Zobin, *J. Phys. F* **7**, 337 (1977).
- <sup>5</sup>E. Callen, Y. J. Liu, and J. R. Cullen, *Phys. Rev. B* **16**, 263 (1977).
- <sup>6</sup>J. D. Patterson, G. R. Gruzalski, and D. J. Sellmeyer, *Phys. Rev. B* **18**, 1377 (1978).
- <sup>7</sup>M. C. Chi and R. Alben, *J. Appl. Phys.* **48**, 2987 (1977); M. C. Chi and T. Egami, *J. Appl. Phys.* **50**, 165 (1979).
- <sup>8</sup>R. Harris and S. H. Sung, *J. Phys. F* **8**, L299 (1978); but see also R. Harris (unpublished).
- <sup>9</sup>A. Aharony, *Phys. Rev. B* **12**, 1038 (1975).
- <sup>10</sup>Y. Imry and S. -K. Ma, *Phys. Rev. Lett.* **35**, 1399 (1976); R. S. Alben, J. J. Becker, and M. C. Chi, *J. Appl. Phys.* **49**, 1653 (1978).
- <sup>11</sup>J. H. Chen and T. C. Lubensky, *Phys. Rev. B* **16**, 2106 (1977).
- <sup>12</sup>S. F. Edwards and P. W. Anderson, *J. Phys. F* **5**, 965 (1975); D. Sherrington and S. Kirkpatrick, *Phys. Rev. Lett.* **35**, 1792 (1975).
- <sup>13</sup>R. A. Pelcovits, E. Pytte, and J. Rudnick, *Phys. Rev. Lett.* **40**, 476 (1978); R. A. Pelcovits, *Phys. Rev. B* **19**, 465 (1979); E. Pytte, *Phys. Rev. B* **18**, 5046 (1978). E. Pytte, to appear in *Ordering in Strongly-Fluctuating Condensed Matter Systems*, edited by T. Riste (Plenum, New York, 1980), Proceedings of a NATO Advanced Study Institute at Geilo, Norway, May 1979.
- <sup>14</sup>A. J. Bray and M. A. Moore, *Phys. Rev. Lett.* **41**, 1069 (1978); *J. Phys. C* **12**, 79, 1349 (1979). A. J. Bray and M. A. Moore, *J. Phys. F* **7**, 1333 (1977); A. J. Bray, M. A. Moore, and P. Reed, *J. Phys. C* **11**, 1187 (1978).
- <sup>15</sup>R. Fisch and A. B. Harris, *Phys. Rev. Lett.* **38**, 785 (1977).
- <sup>16</sup>J. M. D. Coey, T. R. McGuire, and B. Tissier (unpublished). S. von Molnar, C. N. Guy, R. J. Gambino, and T. R. McGuire (unpublished).
- <sup>17</sup>J. M. D. Coey and S. von Molnar, *J. Phys. (Paris)* **39**, L327 (1978).
- <sup>18</sup>G. Toulouse, *Commun. Phys.* **2**, 115 (1977).
- <sup>19</sup>D. C. Mattis, *Phys. Lett. A* **56**, 421 (1976).
- <sup>20</sup>B. Derrida and J. Vannimenus, *J. Phys. (Paris)* (to be published).
- <sup>21</sup>H. Thomas, to appear in *Ordering in Strongly-Fluctuating Condensed Matter Systems*, edited by T. Riste (Plenum, New York, 1980).
- <sup>22</sup>J. M. D. Coey, *J. Appl. Phys.* **49**, 1646 (1978).
- <sup>23</sup>A. A. Migdal, *Zh. Eksp. Teor. Fiz.* **69**, 1457 (1975) [*Sov. Phys. JETP* **42**, 743 (1976)].
- <sup>24</sup>L. P. Kadanoff, *Ann. Phys. (N.Y.)* **100**, 359 (1976).
- <sup>25</sup>S. Kirkpatrick, *Phys. Rev. B* **15**, 1533 (1978).
- <sup>26</sup>J. Vannimenus and G. Toulouse, *J. Phys. C* **10**, L537 (1977); S. Kirkpatrick, *Phys. Rev. B* **16**, 4630 (1977).
- <sup>27</sup>See, e.g., *Monte Carlo Methods in Statistical Physics*, edited by K. Binder (Springer-Verlag, Berlin, 1978).
- <sup>28</sup>S. Kirkpatrick and D. Sherrington, *Phys. Rev. B* **17**, 4384 (1978); R. Palmer and C. M. Pond, *J. Phys. F* **9**, 1451 (1979).
- <sup>29</sup>S. Kirkpatrick and C. M. Varma, *Solid State Commun.* **23**, 687 (1978); A. L. Efros, N. Van. Lien, and B. I. Shklovskii, *J. Phys. C* **12**, 1869 (1979).
- <sup>30</sup>L. E. Wenger and P. H. Keesom, *Phys. Rev. B* **11**, 3497 (1975).
- <sup>31</sup>S. Kirkpatrick (unpublished).
- <sup>32</sup>S. Kirkpatrick, to appear in *Ordering in Strongly-Fluctuating Condensed Matter Systems*, edited by T. Riste (Plenum, New York, 1980).